Geometric and electronic structure of closed-shell bimetallic A_4B_{12} clusters

Yan Sun[1] and René Fournier[2,*]
[1]*Department of Physics, York University, Toronto, Ontario, Canada M3J 1P3*
[2]*Department of Chemistry, York University, Toronto, Ontario, Canada M3J 1P3*
(Received 24 May 2006; published 29 June 2007)

We studied, by density functional theory, a group of 16 clusters having the general formula A_4B_{12}, where "*A*" is divalent and "*B*" monovalent. Global optimization was done in each case followed by calculation of energy second derivatives and vibrational frequencies. The clusters have large highest occupied molecular orbital-lowest unoccupied molecular orbital gaps ranging from 1.2 to 2.6 eV and other features suggesting special stability. This is consistent with the jellium model and 20 electron count. A T_d symmetry cage structure is found as the putative global minimum for Mg_4Ag_{12}, Mg_4Au_{12}, Cd_4Au_{12}, and Ca_4Na_{12}. It is also a low energy isomer (less than 0.1 eV above the global minimum) for Zn_4Au_{12}, Be_4Au_{12}, and Be_4Ag_{12}. The T_d cage structure has ions arranged in shells, with charge +8 and +12, that match two jellium electronic shell closings, $(1s^2,1p^6)$ and $(1d^{10},2s^2)$ with 8 and 12 electrons, respectively. The importance of symmetry and ion shells is shown by the relative stability of homotops of Mg_4Ag_{12}.

DOI: 10.1103/PhysRevA.75.063205 PACS number(s): 36.40.Qv

Stable clusters [1,2], and clusters stabilized by addition of ligands [3], deserve attention because they are unusual species, often highly symmetric, and they are potential building blocks for new materials. Clusters of most elements display so-called magic numbers at specific nuclearities. These clusters are relatively stable within their respective series; but the vast majority of magic clusters, fullerenes being one exception, are not truly stable. They react or coalesce under normal conditions and fail to make the "gigantic leap from beams to beakers" [1]. They cannot be isolated or used in chemical syntheses, but are interesting, nevertheless, because they point to factors that determine cluster stability. Some magic clusters owe their stability to the closing of an atomic shell [4], others to the closing of an electronic shell [5,6]. Other factors have been invoked to explain the relative stability of elemental clusters, including orbital symmetry, the presence of stable subunits, and minimization of strain and surface energy. Analysis of the relative energies of metal cluster isomers shows that those factors often counteract each other [7–9]. Very few clusters, even among magic clusters, satisfy all of the stability criteria simultaneously. Those few that satisfy more than one criterion, like Al_{13}^-, do possess unusual stability [10]. When clusters contain two or more elements the number of possible combinations increases a lot. This creates an opportunity, maybe, to find species that satisfy more stability criteria than elemental clusters, and yet retain some of the features that make clusters different from molecules and passivated nanoclusters.

Here we report calculated properties for a series of A_4B_{12} (*A* is divalent, *B* is monovalent) tetrahedral clusters that satisfy many stability criteria: they have high symmetry, closed atomic and electronic shells (20 electrons), and small strain. They fall in the category of doubly magic clusters, i.e., stability is expected on account of both electronic and atomic shells [11]. They are bimetallic analogs of tetrahedral clusters discussed by Reimann *et al.* [12], and as such, they have an additional interesting feature: their ions are arranged in shells with charges that add up to $q_1=+8$ and $q_2=+12$, and this matches *two* magic numbers of the jellium model, 8 and $8+12=20$. So in a sense, these clusters are "triply magic": closed atomic shells, closed electronic shells, and coincident ionic and electronic shells. We stress, however, that despite satisfying many stability criteria, all magic metal clusters are probably unstable with respect to coalescence or other simple reactions. Indeed, in 9 cases out of 16, we find that the high symmetry triply magic structure is not even a likely candidate for the global minimum (GM). Further, we report estimates of dimerization energies that are large and negative suggesting that all A_4B_{12} clusters are unstable with respect to dimerization. Previous calculations [13] also led to conclude that stable (under normal conditions) *small and unpassivated* metal clusters are unlikely to exist. Still, the relative stability of magic clusters is interesting for theory and is relevant for cluster beam experiments where it manifests itself by peaks in relative cluster abundances.

We used the GAUSSIAN03 software [14] and did Kohn-Sham density functional theory (KSDFT) calculations at the B3LYP (gradient corrected hybrid functional) and VWN (local spin density) levels of theory with LANL2DZ basis sets. We used B3LYP because it gives more accurate band gaps than other DFT methods [15]. However, cohesive energies of metallic systems may not be as accurate with B3LYP, so we also did calculations with the well-known VWN functional. For each *A*-*B* element combination considered, we did a local optimization and characterization of the T_d symmetry structure having a central A_4 tetrahedron and 12 symmetrically placed *B* atoms. We also performed global optimization for every *A*-*B* combination by Tabu search in descriptor space (TSDS) [16] with energy evaluated with GAUSSIAN03 and the VWN functional. Briefly, a TSDS optimization proceeds as follows. In each cycle, many geometric structures ("candidate" structures) are generated randomly, from scratch or by modification of one of the structures of a pre-

*renef@yorku.ca

TABLE I. HOMO-LUMO gap (E_g), lowest vibrational frequency (ω_{min}), ionization energy (IE), electron affinity (EA), and excitation energy to the lowest triplet state (E_t) for the global minimum of A_4B_{12} clusters.

A_4B_{12}	E_g (eV)	ω_{min} (cm^{-1})	IE (eV)	EA (eV)	E_t (eV)
Be_4Au_{12}	2.598	15	7.068	2.098	1.0
Mg_4Ag_{12}	2.463	37	6.085	1.209	0.6
Zn_4Ag_{12}	2.318		6.062	1.467	1.20
Mg_4Au_{12}	2.284	34	6.550	1.881	0.9
Be_4Cu_{12}	2.269	33	5.985	1.239	1.30
Zn_4Cu_{12}	2.258	27	6.055	1.297	1.10
Zn_4Au_{12}	2.144	20	6.459	2.015	0.81
Cd_4Ag_{12}	2.010	28	5.896	1.655	0.88
Be_4Ag_{12}	1.982	26	5.738	2.724	0.9
Zn_4Li_{12}	1.805	39	4.562	0.610	0.7
Cd_4Au_{12}	1.777	28	6.368	2.213	0.13
Ca_4Na_{12}	1.638	44	3.793	0.588	0.77
Cd_4Cu_{12}	1.546	14	5.509	1.688	0.7
Zn_4Na_{12}	1.507	20	3.810	0.705	0.5
Mg_4Na_{12}	1.348	6	3.661	0.767	0.4
Mg_4Li_{12}	1.209	76	4.094	0.968	0.33

TABLE II. HOMO-LUMO gap (E_g), lowest vibrational frequency (ω_{min}), ionization energy (IE), electron affinity (EA), and atomic exchange energy (E_{ex}) of the T_d A_4B_{12} clusters, and their energy relative to the global minimum structure (RE).

A_4B_{12}	E_g (eV)	ω_{min} (cm^{-1})	IE (eV)	EA (eV)	E_{ex} (eV)	RE (eV)
Be_4Cu_{12}	2.583	12	6.402	1.335	3.060	0.438
Mg_4Ag_{12}	2.463	37	6.085	1.209	1.829	0
Zn_4Au_{12}	2.316	25	6.914	2.218	1.183	0.093
Be_4Au_{12}	2.302	12	7.015	2.262	5.017	0.055
Mg_4Au_{12}	2.284	34	6.550	1.881	2.157	0
Be_4Ag_{12}	2.156	11	5.795	1.291	3.600	0.012
Zn_4Ag_{12}	2.145	27	5.421	1.494	0.488	0.528
Zn_4Cu_{12}	1.952	38	5.584	1.290	0.477	1.898
Cd_4Ag_{12}	1.851	20	5.541	1.501	0.05	0.504
Cd_4Au_{12}	1.777	28	6.368	2.213	0.351	0
Mg_4Li_{12}	1.749	95	4.430	0.743	1.801	0.268
Zn_4Li_{12}	1.720	27	4.437	0.864	1.300	0.951
Mg_4Na_{12}	1.716	4	4.044	0.727	1.036	0.362
Cd_4Cu_{12}	1.648	16	5.284	1.323	0.419	1.907
Ca_4Na_{12}	1.638	44	3.793	0.588	1.136	0
Zn_4Na_{12}	1.606	29	4.243	0.803	0.652	0.492

vious cycle. The $A-A$, $B-B$, and $A-B$ bond lengths in candidate structures are set at predefined values that are typical for local energy minima of A_xB_y. Geometric descriptors, such as moments of inertia and mean atomic coordination, are computed for all candidate structures. A model energy is calculated for each candidate by interpolation over the DFT energies of previous structures, using descriptors as interpolation variables. Next, a score is assigned to each candidate based on both the model energy and an index expressing the degree of similarity to previous structures. The best candidates are those that combine a low model (or "predicted") energy and a low similarity to previous structures. In our calculations, only one out of 100 candidate structures is retained in each cycle: this structure is passed over to the Gaussian software for an accurate energy calculation, and the result goes into a growing list of (structure, energy) data. In the early stages, the selection process favors dissimilar structures (exploration), while in later stages there is gradually more emphasis put on the energy (intensification). After N cycles, the first part of TSDS ends: a new score based on KSDFT energy and similarity is calculated for all N cases, structures are ordered according to this score, and the M best are passed over to the Gaussian software for local optimization. In our runs we used $N=800$ and $M=15$. So each TSDS run generated 800 qualitatively different structures and had a total of roughly $800+15\times50=1550$ energy evaluations. The best structure among the 15 VWN local minima was then used as input for a final B3LYP local optimization. The properties calculated by B3LYP for that final structure are the ones reported in Tables I and II and elsewhere, unless specified otherwise. All calculations were done on singlet spin states except for a few tests on higher spin multiplicities which we describe later.

The GM predicted by TSDS are depicted in Fig. 1. The T_d symmetry structure, which shows up among the GM of Fig. 1, is shown again in two other views in Fig. 2. Depending on the A-A distance in the inner tetrahedron, this structure can be viewed either as a truncated tetrahedron (i.e., like Au_{20} [18] with four missing atoms) or as a cage. We studied this structure for all A_4B_{12} clusters and, for Mg_4Ag_{12}, we also did calculations on several homotops obtained by permutation of atoms (see Fig. 3).

Our main results are in Table I where predicted GM of the clusters are arranged in decreasing order of their gap between highest occupied molecular orbital (HOMO) and lowest unoccupied molecular orbital (LUMO), E_g. All clusters, with the possible exception of Zn_4Ag_{12} [19], are true minima, their ω_{min} is real (but barely so for Mg_4Na_{12}). All but two of the E_g's are larger than 1.5 eV which is quite large for metal clusters of that size. We also calculated E_g for elemental clusters A_{16} and B_{16} in the T_d geometry for comparison and found E_g's that range from 0.26 to 0.47 eV. This shows the importance of the valence electron count. We can also compare the E_g's of Table I to the largest HOMO-LUMO gaps calculated of any metal cluster of comparable size in the literature. In making these comparisons, two things should be kept in mind. First, E_g generally gets larger as the number of atoms goes down. Second, for a given cluster, B3LYP gives a value of E_g that is typically larger

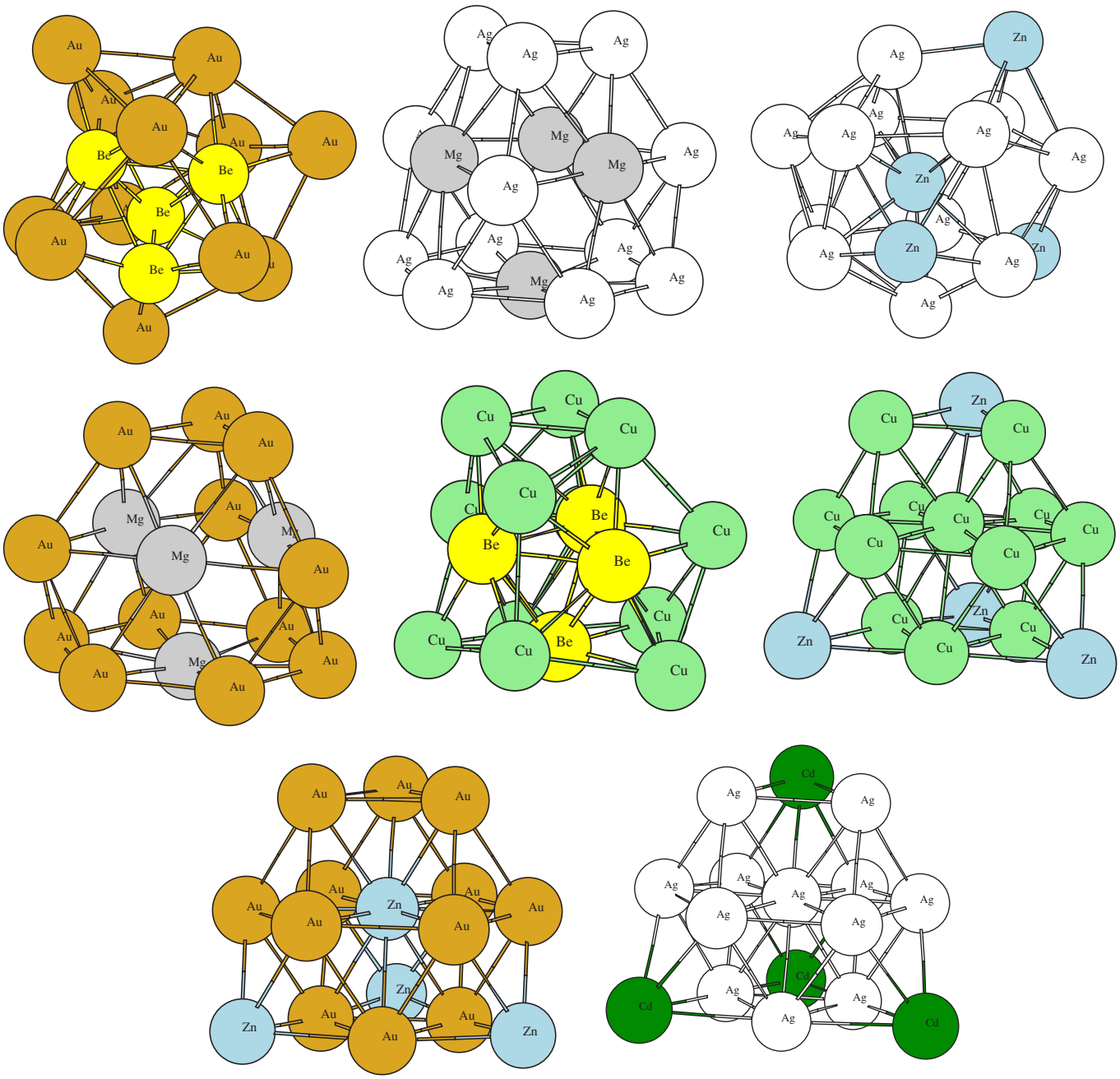

FIG. 1. (Color online) Global minima of A_4B_{12} clusters found by TSDS optimization on the VWN energy surface. A and B elements are (a) BeAu, (b) MgAg, (c) ZnAg, (d) MgAu, (e) BeCu, (f) ZnCu, (g) ZnAu, (h) CdAg, (i) BeAg, (j) ZnLi, (k) CdAu, (l) CaNa, (m) CdCu, (n) ZnNa, (o) MgNa, and (p) MgLi.

than local spin-density (LSD) theory by 20–40%, except in cases where the LSD gap is very small. Some of the largest HOMO-LUMO gaps reported for metal clusters of 16 or more atoms are $Ag_{17}Cu_{17}$ (BPW91, 0.97 eV) [17], $Au_{12}Cu_{22}$ (BPW91, 1.06 eV) [20], Au_{20} (BPW91, 2.10 eV) [18,20], and Na_{20} and Mg_{20} (B3LYP, 1.6 and 1.5 eV, respectively) [24]. The largest E_g of metal clusters with fewer than 16 atoms are found mostly among icosahedral 13-atom and related clusters: WAu_{12} (B3LYP, 3.0 eV) [21], $MoCu_{12}$ (LSD, 3.0 eV) [22], $Al_{12}B_2$ (B3LYP, 2.48 eV) [23], $TlPb_{12}$ (B3LYP, 1.80 eV) [25], $AlPb_{12}^+$ (B3LYP, 3.1 eV) [26], and $Al_{13}Ag$ (PW91, 1.78 eV) [27]. Other large gap clusters are Sb_{10} (PBE, 2.00 eV) [28], Pb_4Li_4 and Pb_4Na_4 (LSD, 2.5 eV) [29], and many more smaller clusters. Clearly, Be_4Au_{12} and Mg_4Ag_{12} have a very large gap compared to metal clusters of their size.

Metal clusters often have higher multiplicity ground states. In the case of A_4B_{12} clusters, however, electronic closed shells and the relatively large HOMO-LUMO gaps suggest that the ground states are probably all singlet; but higher spin ground states cannot be ruled out entirely. We did not do an exhaustive search for higher spin ground states of A_4B_{12}, but we performed local optimization on the triplet and quintet energy surfaces of every cluster in Table I using their

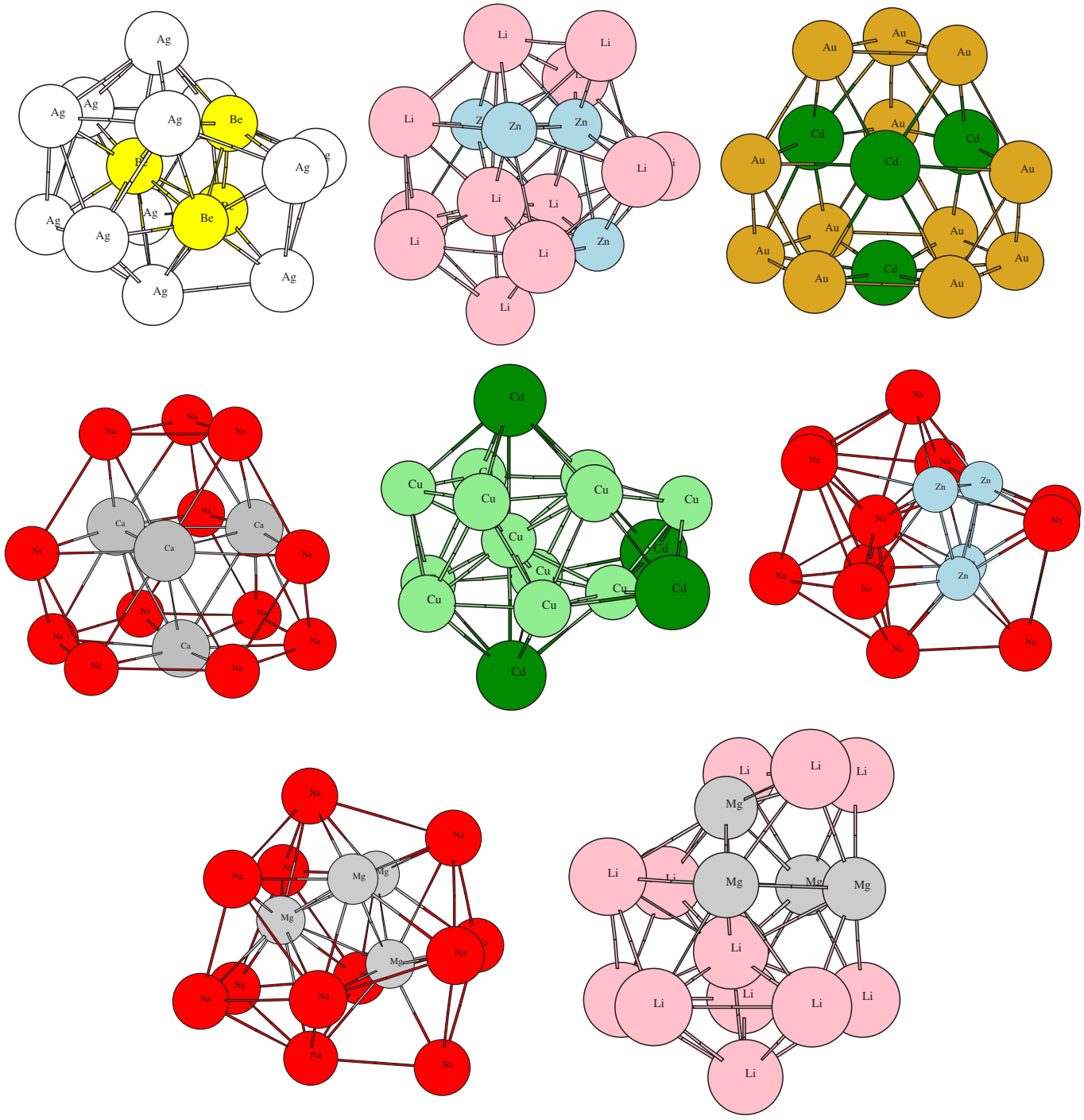

FIG. 1. (*Continued*).

singlet GM as the initial geometry. The rightmost column of Table I shows the energy of the triplet relative to singlet, E_t, obtained in that way. We could not achieve fully self-consistent solutions in some instances. In those cases, energies are shown with only one figure after the decimal point: we think they have an accuracy of ±0.1 eV. We see that E_t is always positive, i.e., the triplet is less stable than the singlet in all cases. The quintet state energies, which are not shown, are significantly larger than triplet energies in every case. There is, as expected, some correlation between E_g and E_t, but it is only a rough correlation. The lowest triplet state, E_t=0.13 eV, is found for Cd_4Au_{12}. It is possible that global search on the triplet energy surface of Cd_4Au_{12} would find a lower energy geometry and maybe yield a triplet GM. It seems unlikely that any of the other clusters would have a triplet or higher spin GM.

Calculated ionization energy (IE) and electron affinity (EA) are more relevant for experiments than E_g and are reported in Tables I and II. There is a correlation between HOMO-LUMO gaps and IE-EA, but it is not perfect. Among clusters of Table II, the root-mean-square deviation (rmsd) between ($2.06E_g$) and IE-EA is 0.14 eV. The large IE-EA of

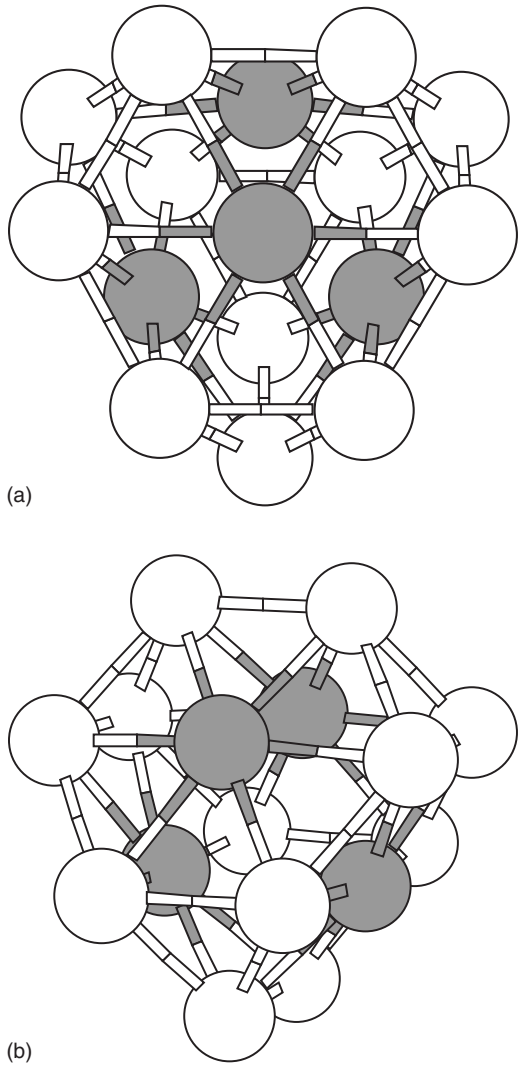

FIG. 2. Structure of A_4B_{12} clusters with four inner shell A atoms and T_d symmetry. (a) top view and (b) side view.

Be_4Au_{12} and Mg_4Ag_{12} should make these clusters unreactive and abundant relative to other clusters in beam experiments. It would be interesting to see photoelectron spectroscopy measurements on a A_4B_{12} cluster anion, like was done for Au_{20}^- [18] and Au_{16}^- [30].

We now turn to Fig. 1 and a comparison of predicted structures for the 16 clusters. They fall into four groups: (a) the T_d cage (Mg_4Ag_{12}, Mg_4Au_{12}, Cd_4Au_{12}, Ca_4Na_{12}); (b) the fcc fragment (Zn_4Cu_{12}, Zn_4Au_{12}, Cd_4Ag_{12}); (c) the triply capped icosahedron (Be_4Ag_{12}, Mg_4Li_{12}, Zn_4Li_{12}, Cd_4Cu_{12}, Zn_4Na_{12}, Zn_4Ag_{12}); and (d) irregular structures with a compact tetrahedral core (Be_4Au_{12}, Be_4Cu_{12}, Mg_4Na_{12}). Mg_4Na_{12} could also fit in category (c) but with a very distorted Mg-centered icosahedron, and Be_4Ag_{12} may fit in group (d) because it has a tetrahedral Be_4 unit. In Zn_4Ag_{12}, there is no clear distinction between the atoms of the icosahedron and the three capping atoms. That structure is more easily seen as a Zn atom capping an axial arrangement of $Ag/Ag_6/Zn/Ag_4Zn_2/Ag$ where the two six-atom rings are staggered. Staggered six-atom rings are also subunits in GM structures found for Li_n ($n=16$, 17, and 18) clusters [8]. Groups (a) and (b) are void-centered and atom-centered fragments of the fcc crystal structure, respectively. Structure (a) looks more open because the four A atoms have slightly elongated bonds, but if A atoms are considered to be neighbors, then (a) and (b) have essentially the same mean atomic coordination, 6.2. Structure (d) is slightly more compact, with a mean atomic coordination around 6.3, and (c) is more compact still at 6.5.

Structure (a) (Fig. 2) is analogous to the recently proposed "golden cage" Au_{16}^- [30]. It can be derived from the T_d structure of Au_{20} [18] by removing the four apex atoms. Removing these atoms increases the mean atomic coordination and makes the structure rounder. By having four divalent inner shell atoms, the T_d symmetry and electron count of 20 of Au_{20} are preserved. Ideally, for stability, the four inner shell atoms should be smaller or of a comparable size to B and should have a cohesive energy that is not too small. Be_4M_{12} ($M=$Cu, Ag, Au) fits those stability criteria best, but none of them has the cage as its GM, although it is very near to the GM energy for Be_4Ag_{12} and Be_4Au_{12}. Note that the four Be atoms form a compact, more or less central, tetrahedral core in all three Be_4M_{12} structures [Figs. 1(a), 1(e), and 1(i)]. The relative energy (RE) column of Table II shows most of the lowest entries are for Au containing clusters, which confirms gold's propensity to adopt tetrahedral cage structures [30]. These clusters could in principle accommodate an additional atom at the center with only a slight expansion of the A_4 tetrahedron and without disrupting the $A-B$ and $B-B$ bond network. The VWN optimized structures (a) are described in Table III. The geometric parameter r is the ratio of the mean distance to the center of mass of the first and second ion shells. It appears that achieving an optimal r matters for the stability of these clusters because the clusters with the smallest (Cd_4Cu_{12}) and largest (Zn_4Na_{12}) value of r have the smallest HOMO-LUMO gap and large RE (Table II). Clusters whose GM is the T_d structure have r values in the range from 1.57 to 1.78. The mean distance (in Å) between pairs of neighboring $A-A$ and $B-B$ atoms are denoted by d_{AA} and d_{BB}. It should be noted that Be_4Ag_{12} and Cd_4Cu_{12} have severely distorted geometries and Zn_4Ag_{12} is slightly distorted.

We now discuss the stability of the cage A_4B_{12} clusters. One stability criterion for clusters is the energy of reactions like these:

$$2A_4B_{12} \rightarrow A_4B_{11} + A_4B_{13},$$

$$2A_4B_{12} \rightarrow A_3B_{12} + A_5B_{12}.$$

The first reaction produces species with odd numbers of electrons so it surely must give large positive energies of reaction. We define the atom exchange energy, E_{ex}, as the energy for the *second* reaction, which involves only species with even numbers of electrons, and where reactants and products have the T_d structure or a local minimum found after adding or removing an atom from a T_d structure. *A priori*, one might expect E_{ex} to be sometimes negative and sometimes positive and generally small in absolute value; but we find that E_{ex} is always large and positive (Table II). It is typically 2/3 of the

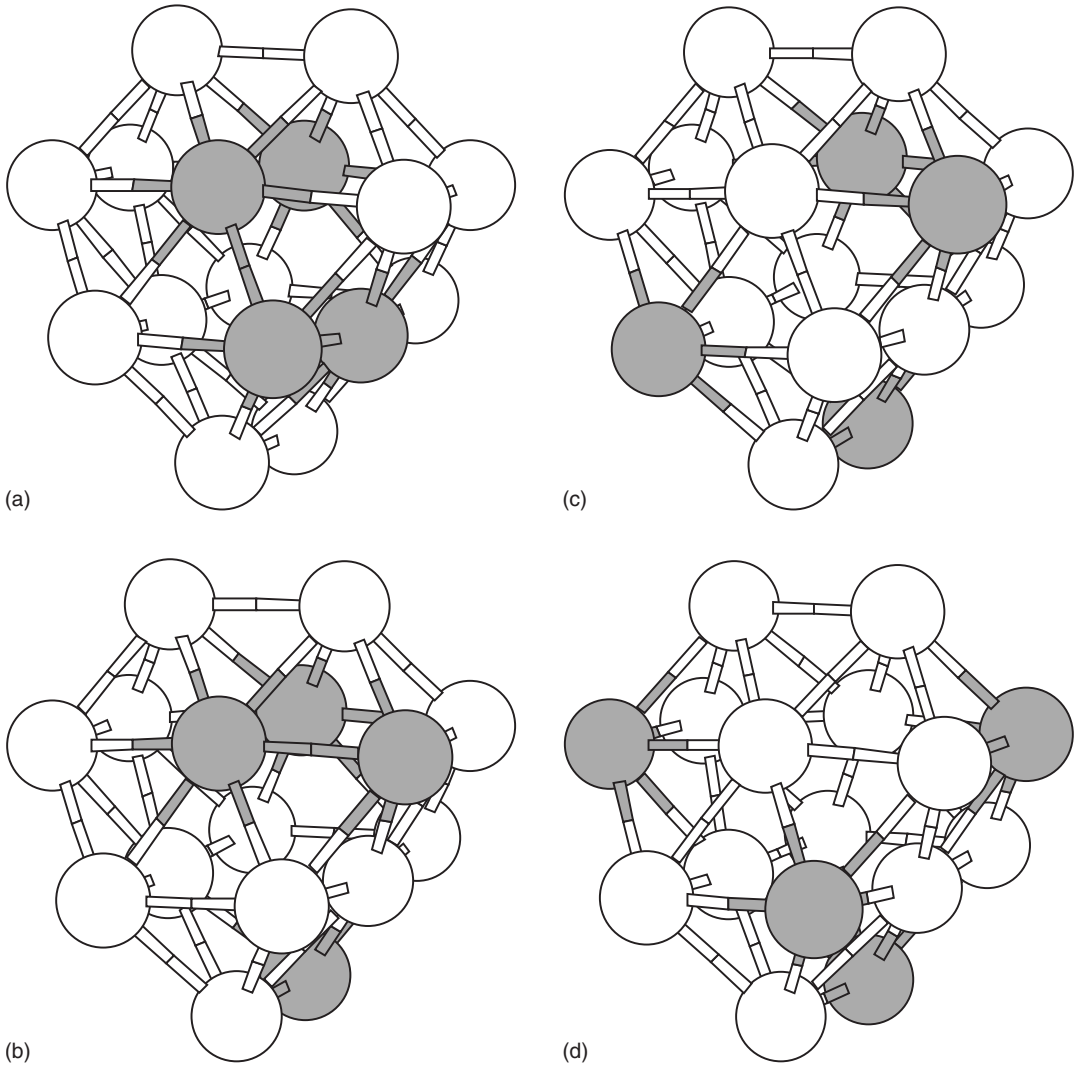

FIG. 3. Most stable homotop of Mg_4Ag_{12} among those having: (a) three inner shell Mg atoms; (b) two inner shell Mg atoms; (c) one inner shell Mg atom; and (d) no inner shell Mg atom.

weighted average of the experimental cohesive energies of the two metals. The fact that $E_{ex}>0$ for Zn_4Cu_{12}, Zn_4Ag_{12}, and Cd_4Cu_{12} itself is surprising considering that the reaction results in moving an atom of the low cohesive energy element to the outer shell and an atom of the high cohesive energy element to the inner shell. E_{ex} is particularly large in Be_4M_{12} (M=Cu, Ag, Au) which is understandable considering that Be has a much larger surface energy than Mg, Zn, and Cd.

Another reaction that can destroy clusters, and is useful in quantifying their stability, is dimerization: $2\ A_4B_{12}\rightarrow A_8B_{24}$. We cannot directly calculate energies of dimerization such as $2\ Mg_4Ag_{12}\rightarrow Mg_8Ag_{24}$ because global optimization of Mg_8Ag_{24} at the DFT level is beyond our current capabilities. However, we can make a *rough estimate* as follows. We assume that the energy for the dimerization reaction has two main contributions: (a) a negative surface energy term ΔE_s which comes about because a $2N$-atom spherical cluster has roughly $2^{-1/3}$ as much surface area as two N-atom spherical clusters; and (b) a "shell" term ΔE_e originating from details of the atomic and electronic structure. In our case, ΔE_e is expected to be positive because, although Mg_8Ag_{24} has 40

TABLE III. Geometric parameters (see text) of VWN-optimized T_d A_4B_{12} clusters.

A:	Be	Mg	Zn	Be	Mg	Be	Zn	Zn	Cd	Cd	Mg	Zn	Mg	Cd	Ca	Zn
B:	Cu	Ag	Au	Au	Au	Ag	Ag	Cu	Ag	Au	Li	Li	Na	Cu	Na	Na
r	1.91	1.64	1.73	2.03	1.64	2.01	1.70	1.49	1.56	1.57	1.78	1.84	2.02	1.32	1.78	2.14
d_{AA}	2.34	3.21	3.01	2.30	3.20	2.28	3.06	3.15	3.43	3.40	3.23	2.98	3.33	3.66	4.11	3.07
d_{BB}	2.33	2.76	2.72	2.82	2.75	2.80	2.72	2.45	2.78	2.78	3.00	2.87	3.52	2.49	3.81	3.44

TABLE IV. Energies (in eV) of Mg_4Ag_{12} homotops relative to the structure with no outer shell Mg atom ($n=0$). The average values of E_g for homotops with n outer shell Mg atoms are, in eV, 2.46 ($n=0$), 2.09 ($n=1$), 2.00 ($n=2$), 1.99 ($n=3$), and 1.96 ($n=4$).

$n=1$	0.16	0.30	0.39			
$n=2$	0.54	0.83	1.00			
$n=3$	0.70	0.75	0.77	0.80	0.94	1.41
	1.52	1.52				
$n=4$	1.08	1.19	1.21	1.26	1.36	1.37
	1.40	1.46	1.47	1.49	1.51	

electrons which also corresponds to a jellium electronic shell closing, it may not have the high symmetry and matching electronic and atomic shells of Mg_4Ag_{12}. We expect that ΔE_e should be roughly twice a typical homotop energy (Table IV), or, $\Delta E_e \approx +0.6$ to +2.4 eV. We calculated a *model* surface energy for Mg_4Ag_{12} by the "SEM" model described below. It is 30.4 eV. Then, $\Delta E_s \approx (2^{2/3}-2)\times 30.4$ eV $= -12.6$ eV. By this estimate, we predict that Mg_4Ag_{12} would dimerize with a very large negative energy of reaction, at least −10 eV. Even a cluster with a small surface energy like Ca_4Na_{12} is predicted to show a large decrease of surface energy upon dimerization, roughly −6 eV, and this would surely offset any energy term associated with shell closings. Therefore we think that unpassivated metal clusters, magic or not, are probably all *thermodynamically* unstable with respect to dimerization. There is still a possibility that some clusters may be metastable, in particular those having a large E_g and large E_{ex}. These stability indicators could be linked to having closed shells for both atoms and electrons. Indeed the E_g's of the T_d isomers are, on average, slightly larger than the E_g's of the GM (1.995 vs 1.948 eV). Further, Table IV demonstrates the importance for stability of symmetry and matching ionic and electronic shells. It shows the relative energies of 25 homotops of Mg_4Ag_{12}. All homotops have the same basic tetrahedral structure and 20 electron count. They differ only in how sites are occupied in the basic structure and in details that result from their geometry optimization. The atomic radii of Mg and Ag are not too different and cannot account for any big variation of energies among homotops. The cohesive energy and surface energy of Ag are much bigger than for Mg, which suggests that the energy should *decrease* as the number of outer shell Mg atoms increases. But Table IV shows the opposite. The energy is lowest for the homotop with four inner shell Mg atoms, and gradually increases as more Ag atoms occupy the inner shell. A possible explanation for this is based on the matching of atomic and electronic shells. In the jellium model [5], extra stability is associated with electron counts of 2, 8, 20, 40, …, or shells containing 2, 6, 12, 20, … electrons. If this electronic shell structure is approximately valid in a 20-electron metal cluster, the 20 valence electrons exert a force on ions that drives them to adopt a (2,6,12) shell structure in order to give approximate local charge neutrality everywhere. This is analogous to the deformation of jellium spheres (and alkali metal clusters) when a jellium electronic shell is partially filled, an effect which Manninen explained in terms of electrostatic energy [6]; but constraints on the ions geometry prevent a high-symmetry (2,6,12) arrangement. The (8,12) shell structure, however, can be realized. The only homotop of Mg_4Ag_{12} that has this structure is the one with lowest energy. The others have ionic charges in the first shell that add up to +7 or less, and many of them lack the approximate spherical symmetry also required to give a good shell structure. Table IV shows that, on average, as the distribution of ionic charges gets further away from (8,12), the energy increases and the HOMO-LUMO gap decreases.

Another way to assess the importance of shells for cluster stability is to compare atomization energies (AE) calculated by first principles to those calculated with a simple model that ignores electronic structure entirely. We define a surface energy model (SEM) for estimating atomization energies of clusters in the following way. We imagine the surface defined by overlapping spheres of radius $R_j=1.7R_M(j)$, where $R_M(j)$ is the metallic radius of a given element, centered around each atom j. The factor 1.7 is arbitrary, but it is close on average to the ratio of the van der Waals and covalent (or metallic) radius of elements, so it is appropriate for calculating a model molecular surface area. For each atom in the cluster, we generate a fine grid of N points (typically $N=10\,000$) located at the surface of its atomic sphere. We compute the fraction f_j of points on atom j's sphere that do not lie inside any other atomic sphere. The contribution of atom j to the surface area is $a_j=f_j 4\pi R_j^2$. We can normally get this with an accuracy better than 1% for $N=10\,000$. There is an empirical relation between the cohesive energy and surface energy of metals [31]: on a per-atom basis, and for close-packed surfaces, the surface energy is *roughly* 0.16 times the cohesive energy. If we use $R_j=1.7R_M(j)$, we reproduce this empirical relation by setting

$$e_j = 0.878 f_j U_j,$$

TABLE V. Atomization energy (AE, eV) of A_4B_{12} global minima (GM) calculated by VWN, and a simple surface energy model (SEM).

A:	Be	Mg	Zn	Be	Mg	Be	Zn	Zn	Cd	Cd	Mg	Zn	Mg	Cd	Ca	Zn
B:	Cu	Ag	Au	Au	Au	Ag	Ag	Cu	Ag	Au	Li	Li	Na	Cu	Na	Na
VWN	50.1	36.1	43.1	51.4	46.6	41.7	34.2	42.9	32.8	40.6	19.8	19.3	13.9	41.1	13.2	12.9
SEM	41.4	30.4	38.0	44.0	37.5	37.3	30.4	36.3	30.0	36.0	18.9	18.3	14.5	36.5	15.3	14.0
VWN/SEM	1.21	1.19	1.13	1.17	1.24	1.12	1.13	1.18	1.10	1.13	1.05	1.05	0.96	1.13	0.86	0.92

TABLE VI. Atomization energy (AE, eV) of A_4B_{12} calculated by B3LYP, VWN, and a simple surface energy model (SEM) for the T_d structures.

A:	Be	Mg	Zn	Be	Mg	Be	Zn	Zn	Cd	Cd	Mg	Zn	Mg	Cd	Ca	Zn
B:	Cu	Ag	Au	Au	Au	Ag	Ag	Cu	Ag	Au	Li	Li	Na	Cu	Na	Na
B3LYP	31.4	21.1	27.2	32.2	29.4	24.9	17.9	23.8	16.4	22.2	13.9	12.0	8.5	21.5	8.3	7.0
VWN	50.4	36.1	43.0	51.4	46.6	42.1	33.9	41.6	32.8	40.6	20.1	18.8	13.9	38.5	13.2	12.4
SEM	41.3	30.4	36.4	44.3	37.5	37.4	29.3	34.2	28.1	36.0	18.7	18.2	15.1	34.0	15.3	14.1
B3LYP/SEM	0.76	0.69	0.75	0.73	0.78	0.66	0.61	0.66	0.58	0.62	0.74	0.66	0.51	0.71	0.54	0.50
VWN/SEM	1.22	1.19	1.18	1.16	1.24	1.13	1.16	1.22	1.17	1.13	1.08	1.03	0.92	1.13	0.86	0.88

where e_j is atom j's contribution to the surface energy and U_j is the cohesive energy for that element. Thus we can calculate a surface area A, a surface energy E_s, and atomization energy AE for clusters of any composition and structure:

$$A = \sum_j a_j,$$

$$E_s = \sum_j e_j,$$

$$AE = \sum_j (U_j - e_j).$$

Tables V and VI show AEs calculated by VWN, SEM, and B3LYP (Table VI only). On average, VWN values of AE are 10% larger, and B3LYP values 35% smaller, than SEM. In an absolute sense the SEM probably gives AEs closest to the exact values; but only a quantum method like VWN or B3LYP can reveal variations in stability caused by the clusters' electronic and atomic structure. The ratios of AEs VWN/SEM are most useful. They are generally larger for the clusters with the largest E_g, for both the GM and T_d structures. In some of the cases, differences in surface energies (SEM) may explain why the T_d structure is not the GM. Specifically, there are large differences in SEM energies that disfavor the T_d structure in five cases: Zn_4Ag_{12}, Zn_4Cu_{12}, Cd_4Ag_{12}, Cd_4Cu_{12}, and Zn_4Au_{12}. There are correspondingly large REs in the first four of those, and a positive but small (0.09 eV) RE for Zn_4Au_{12}. Conversely, two of the three clusters that have the T_d structure as a low-lying isomer have a small difference in SEM energies (Be_4Au_{12}, Be_4Ag_{12}), Zn_4Au_{12} being the odd one out. However, note that among Au containing clusters, Zn_4Au_{12} is the one for which the T_d structure is the least stable.

In summary, theoretical arguments based on the jellium model and properties calculated by KSDFT suggest that bimetallic clusters having the composition A_4B_{12} and 20 valence electrons have a large HOMO-LUMO gap and are relatively stable. Among those, Be_4Au_{12} and Mg_4Ag_{12} appear to be the most stable. A high symmetry T_d structure made of two shells of ions is the predicted global minimum of Mg_4Ag_{12} and is a low lying energy isomer (+0.06 eV) for Be_4Au_{12}. Five other clusters have this structure as their global minimum or a low-lying isomer. We believe that the stability of this structure is caused partly by symmetry, and partly by having coincident electronic and ionic shells.

This work was made possible by the facilities of the Shared Hierarchical Academic Research Computing Network (SHARCNET:www.sharcnet.ca) and support by the Natural Sciences and Engineering Research Council of Canada.

[1] A. W. Castleman, Jr. and K. H. Bowen Jr., J. Phys. Chem. **100**, 12911 (1996).
[2] W. Kratchmer, L. D. Lamb, K. Fostiropoulos, and D. R. Huffman, Nature (London) **347**, 354 (1990); S. F. Cartier, Z. Y. Chen, G. J. Walder, C. R. Sleppy, and A. W. Castleman, Jr., Science **260**, 95 (1993).
[3] J. C. Love, L. A. Estroff, J. K. Kriebel, R. G. Nuzzo, and G. M. Whitesides, Chem. Rev. (Washington, D.C.) **105**, 1103 (2005).
[4] T. P. Martin, Phys. Rep. **273**, 199 (1996).
[5] W. D. Knight, K. Clemenger, W. A. deHeer, W. A. Saunders, M. Y. Chou, and M. L. Cohen, Phys. Rev. Lett. **52**, 2141 (1984); W. A. DeHeer, Rev. Mod. Phys. **65**, 611 (1993); M. Brack, *ibid.* **65**, 677 (1993).
[6] M. Manninen, Phys. Rev. B **34**, 6886 (1986).
[7] R. Fournier, J. Chem. Phys. **115**, 2165 (2001).
[8] R. Fournier, J. B. Y. Cheng, and A. Wong, J. Chem. Phys. **119**, 9444 (2003).
[9] Y. Sun and R. Fournier, Chin. Phys. **1**, 210 (2005).
[10] R. E. Leuchtner, A. C. Harms, and A. W. Castleman, Jr., J. Chem. Phys. **91**, 2753 (1989).
[11] S. N. Khanna and P. Jena, Phys. Rev. Lett. **69**, 1664 (1992).
[12] S. M. Reimann, M. Koskinen, H. Häkkinen, P. E. Lindelof, and M. Manninen, Phys. Rev. B **56**, 12147 (1997).
[13] H. Häkkinen and M. Manninen, Phys. Rev. Lett. **76**, 1599 (1996).
[14] M. J. Frisch *et al.*, GAUSSIAN 03, Revision C.02 (Gaussian Inc., Wallingford, CT, 2004).
[15] J. Muscat, A. Wander, and N. M. Harrison, Chem. Phys. Lett. **342**, 397 (2001); K. N. Kudin, G. E. Scuseria, and R. L. Martin, Phys. Rev. Lett. **89**, 266402 (2002).

[16] J. Chen and R. Fournier, Theor. Chem. Acc. **112**, 7 (2004).
[17] G. Rossi, A. Rapallo, C. Mottet, A. Fortunelli, F. Baletto, and R. Ferrando, Phys. Rev. Lett. **93**, 105503 (2004).
[18] J. Li, X. Li, H.-J. Zai, and L.-S. Wang, Science **299**, 864 (2003).
[19] Despite many attempts, we were unable to carry calculations of vibrational frequencies to completion for this particular cluster. The second lowest isomer of Zn_4Ag_{12} is 0.11 eV higher in energy and was verified to be a true minimum (lowest frequency, 32 cm^{-1}). In our experience with TSDS and metal clusters, a local minimization that uses as its initial guess the lowest energy structure of TSDS rarely converges to a higher order critical point of the potential surface. So the structure that we report for Zn_4Ag_{12} is likely a minimum.
[20] R. Ferrando, A. Fortunelli, and G. Rossi, Phys. Rev. B **72**, 085449 (2005).
[21] P. Pyykkö and N. Runeberg, Angew. Chem., Int. Ed. **41**, 2174 (2002).
[22] Q. Sun, X. G. Gong, Q. Q. Zheng, D. Y. Sun, and G. H. Wang, Phys. Rev. B **54**, 10896 (1996).
[23] J. Wan and R. Fournier, J. Chem. Phys. **119**, 5949 (2003).
[24] A. Lyalin, I. A. Solov'yov, A. V. Solov'yov, and W. Greiner, Phys. Rev. A **67**, 063203 (2003).
[25] D. L. Chen, W. Q. Tian, W.-C. Lu, and C.-C. Sun, J. Chem. Phys. **124**, 154313 (2006).
[26] S. Neukermans, E. Janssens, Z. F. Chen, R. E. Silverans, P. v. R. Schleyer, and P. Lievens, Phys. Rev. Lett. **92**, 163401 (2004).
[27] V. Kumar and Y. Kawazoe, Phys. Rev. B **64**, 115405 (2001).
[28] X. Zhou, J. Zhao, X. Chen, and W. Lu, Phys. Rev. A **72**, 053203 (2005).
[29] J. A. Alonso, Nanotechnology **13**, 253 (2002).
[30] S. Bulusu, L.-S. Wang, and X. C. Zeng, Proc. Natl. Acad. Sci. U.S.A. **103**, 8326 (2006).
[31] G. A. Somorjai, *Introduction to Surface Chemistry and Catalysis* (Wiley, New York, 1994).